

# Multi-Orbital Hubbard Model in Infinite Dimensions: Quantum Monte Carlo Calculation

J. E. Han<sup>a</sup>, M. Jarrell<sup>b</sup>, D. L. Cox<sup>c</sup>

<sup>a</sup>-Max-Planck Institut für Festkörperforschung, Heisenbergstr.1, D-70569, Stuttgart, Germany

<sup>b</sup>-Department of Physics, University of Cincinnati, Cincinnati, Ohio 45221

<sup>c</sup>-Department of Physics, University of California, Davis, California 95616

Using Quantum Monte Carlo we compute thermodynamics and spectra for the orbitally degenerate Hubbard model in infinite spatial dimensions. With increasing orbital degeneracy we find in the one-particle spectra: broader Hubbard bands (consistent with increased kinetic energy), a narrowing Mott gap, and increasing quasi-particle spectral weight. In opposition, Hund's rule exchange coupling decreases the critical on-site Coulomb energy for the Mott transition. The metallic regime resistivity for two-fold degeneracy is quadratic-in-temperature at low temperatures.

75.30.Mb, 71.27.+a, 75.10.Dg

The Hubbard Hamiltonian, the simplest model for strongly interacting many-electron systems, has been extremely popular in that, despite its simplicity, the model is considered to capture essential physics in electronic systems, ranging from a metal-insulator transition (MIT) and associated antiferromagnetism to possible  $d$ -wave superconductivity. Although most of the real systems displaying these phenomena have orbital degrees of freedom, most theoretical works have concentrated on the orbitally non-degenerate model for simplicity. Recently, with the advent of the colossal magnetoresistance materials [1], the proposed triplet pairing superconductivity in  $\text{Sr}_2\text{RuO}_4$  [2], and alkali-doped fullerenes [3,4], attention has been turned to the multi-orbital Hubbard model (MOHM) [5,8,9].

With on-site orbital degeneracy  $N_{\text{deg}} > 1$ , one has to consider two additional aspects of the problem: first, the effect of orbital degrees of freedom on the mobility of electrons and second, the role of on-site exchange interactions between degenerate orbitals. In this paper, we concentrate on the MIT in MOHM motivated particularly by alkali-doped fullerenes,  $A_3\text{C}_{60}$  ( $A=\text{K, Rb, Cs}$  etc.). We have studied the problem using Quantum Monte Carlo in a  $d = \infty$  model on both Bethe and hypercubic lattices, with a focus on dynamical properties (obtained by analytic continuation of imaginary time data using the Maximum Entropy method [MEM]). We present the first systematic calculation of one-electron spectral functions at and away from particle-hole symmetry and the first calculation of the optical conductivity and d.c. resistivity for the two-orbital model.

We find that the upper and lower Hubbard bands display a considerable broadening for  $N_{\text{deg}} = 2, 3$  relative to  $N_{\text{deg}} = 1$ , which supports the idea of Gunnarsson, Koch, and Martin [5] and Lu [6] that orbital degeneracy serves to increase the effective hopping matrix element and thereby mitigate the efficacy of correlations in driving a MIT [7]. We also find that the quasiparticle spectral weight increases with  $N_{\text{deg}}$ . We find that the inclusion of Hund's rule exchange serves to decrease the effective hopping, thereby decreasing again the critical value of on-site Coulomb interaction  $U = U_c$  needed for the MIT,

according to the approximate expression

$$U_c(N_{\text{deg}}, J) \approx \sqrt{N_{\text{deg}}} U_c(1, 0) - N_{\text{deg}} J, \quad (1)$$

where  $J$  is the Hund's rule exchange energy. Finally, we present a calculation of the optical conductivity  $\sigma(\omega, T)$  and resistivity  $\rho(T)$  for the  $N_{\text{deg}} = 2$  case which gives a  $T^2$  behaviour in  $\rho(T)$  for  $T \rightarrow 0$ .

We were motivated to carry out this study by consideration of  $A_3\text{C}_{60}$ . Even though the local density approximation predicted well the band-width and the band-gap of this system, it has been suggested that the strong Coulomb repulsion on the  $\text{C}_{60}$  site could drive the system to a strongly correlated metal or even to a Mott-insulator [7]. Since the band-width of  $A_3\text{C}_{60}$  (0.4 eV) is more than two times smaller than the on-site Coulomb repulsion (1-1.5 eV), one can naively predict that the system should be a Mott-insulator, if interpreted in terms of an orbitally nondegenerate Hubbard model. However, the alkali-doped fullerenes are metals despite the large resistivity at zero temperature [10].

It has been suggested that the metallic  $A_3\text{C}_{60}$  can be understood by introducing orbital degeneracy in the Hubbard model [5,6]. The MIT in the MOHM has been studied by the Gutzwiller approximation [6], where Lu showed that the critical value for the on-site Coulomb repulsion strength  $U_c(N_{\text{deg}})$  for MIT at half-filling increases as  $(N_{\text{deg}} + 1)U_c$  with the orbital degeneracy  $N_{\text{deg}}$ . This explains why alkali-doped fullerenes ( $N_{\text{deg}} = 3$ ) can be metallic despite the large intra-molecular Coulomb repulsion and small conduction band-width [3]. Later, Gunnarsson *et al.* [5] argued that  $U_c(N_{\text{deg}})$  behaves as  $\sqrt{N_{\text{deg}}}$ , in a much weaker fashion than the linear dependency of Ref. [6]. The electron hopping is argued to be effectively enhanced with the orbital degeneracy due to the anti-ferromagnetic correlation between nearest sites, which is also supported by their numerical calculation.

To carry out our studies, we have used the dynamical mean field theory (DMFT) [11], where a lattice Hamiltonian is rigorously mapped to an effective impurity model. This approximation, which is exact for infinite spatial dimension or coordination number, is reasonable for mod-

elling the  $C_{60}$ -derived  $t_{1u}$  band due to the large coordination number, 12, between the  $C_{60}$  molecules located at face-centered-cubic sites. Furthermore, with the on-site Coulomb interaction, the impurity Hamiltonian from the DMFT is expected to retain the essential physics of the MIT. The multi-orbital Hubbard Hamiltonian reads

$$H = -\sum_{ij,m\sigma} \left( t_{ij} c_{im\sigma}^\dagger c_{jm\sigma} + h.c. \right) + \epsilon_d \sum_{im\sigma} n_{im\sigma} + H_C, \quad (2)$$

where  $t_{ij}$  is the hopping matrix element between different sites  $i$  and  $j$ ,  $m$  the orbital index,  $\sigma$  the spin index,  $\epsilon_d$  the  $d$ -level energy as the center of the non-interacting band,  $H_C$  the interaction Hamiltonian for Coulomb energy. For simplicity, we have neglected inter-band hopping since we concentrate on the local properties.

The Coulomb interaction term is written [12] as

$$H_C = (U + J) \sum_m n_{im\uparrow} n_{im\downarrow} + (U - J) \sum_{im < m'\sigma} n_{im\sigma} n_{im'\sigma} + U \sum_{im \neq m'} n_{im\uparrow} n_{im'\downarrow} + J \sum_{m < m'} c_{im\uparrow}^\dagger c_{im'\uparrow}^\dagger c_{im'\downarrow} c_{im\downarrow}. \quad (3)$$

Here, we discard the last term proportional to  $J$  for computational convenience although, for full rotational symmetry, all the terms in the above Hamiltonian are needed. The truncated Hamiltonian still captures the Hund's rule physics, and we believe that the form of Eq. (1) remains valid, possibly with a small correction to the term proportional to  $J$ .

The effective impurity model in the DMFT is studied by the Hirsch-Fye algorithm [13] where the partition function is reformulated using a discrete path integral with an imaginary-time interval which we set to  $\Delta\tau = 1/3$ . For the free density of states (DOS) in the DMFT, a semi-circular DOS (corresponding to the infinite coordination number Bethe lattice),  $D(\epsilon) = \frac{2}{\pi} \sqrt{1 - \epsilon^2}$  with band-width  $W=2$ , is used for calculations of thermodynamic quantities such as occupation numbers. A Gaussian DOS (corresponding to the infinite dimensional hypercubic lattice),  $D(\epsilon) = \frac{1}{\sqrt{\pi}} \exp(-\epsilon^2)$  with  $W=\sqrt{2}$ , is used for one-particle spectral functions. We normalize  $t_{ij} = t$  by  $t = t^*/2\sqrt{d}$ , as the dimensionality  $d$  goes to infinity. All energies here are measured in units of  $t^*$  for the Gaussian DOS, and in units of the bandwidth for the semi-circular DOS.

At  $J = 0$ , we identified the MIT for  $N_{\text{deg}} = 1, 2, 3$  near half-filling by computing the occupation numbers at  $\epsilon_d$  away from the particle-hole symmetric value, *i.e.*,  $\epsilon_d = \epsilon_{ph} + 0.2$  where  $\epsilon_{ph} = (N_{\text{deg}} - \frac{1}{2})U + (1 - \frac{N_{\text{deg}}}{2})J$ . FIG. 1 shows the occupation numbers versus the Coulomb repulsion with the semi-circular DOS. The occupation numbers and the chemical potentials are plotted with respect to the particle-hole symmetric values. The temperatures are at  $T = 1/12, 1/16$ . When the system is insulating with the chemical potential inside an insulating gap, the occupation number does not change with a slight shift of chemical potential from  $\epsilon_{ph}$ . As will be illustrated

later, the Mott insulating-gap manifests as a plateau in  $n_d$  vs  $\epsilon_d$ . The critical Coulomb repulsion,  $U_c$ , is read off from the point where the occupation number  $n_d$  at  $\epsilon_d = \epsilon_{ph} + 0.2$  deviates from  $N_{\text{deg}}$  in FIG. 1.

$U_c(N_{\text{deg}})$  increases with the orbital degeneracy, in agreement with Ref. [5], although the data are not sufficiently precise to conclude that the insulating gap is proportional to  $\sqrt{N_{\text{deg}}}$  from small  $N_{\text{deg}}$  and  $U/W$ . For  $N_{\text{deg}} = 3$ , the occupation numbers have not fully converged yet for  $T = 1/16$  and we obtain  $U_c/W \geq 2.3$ . Compared with  $A_3C_{60}$ , this value of  $U_c$  puts the experimental ratio near the edge of MIT transition. Therefore, it is theoretically possible, if not decisively proven, that  $A_3C_{60}$  can be described as a strongly correlated metal despite being at half filling.

The QMC Green's function along imaginary time is analytically continued for the one-particle spectral function by MEM [14]. One-particle spectral functions at and away from half-filling are shown in FIG. 2 when  $T = 1/12$  and  $J = 0$ . In plot (a), at half-filling, the upper (UHB) and lower Hubbard bands (LHB) are split by the Coulomb interaction strength  $U$ . Note that the width of these peaks increases with the orbital degeneracy, in the same fashion that the electron hopping is enhanced for conduction of the charge excitation. For the non-degenerate model ( $N_{\text{deg}} = 1$ ), the spectral weight at zero frequency is very small, hence a sign of an insulating pseudo-gap (the system cannot become a true insulator due to the non-vanishing tail of the Gaussian free DOS). With increasing  $N_{\text{deg}}$ , the MOHM evolves to solutions with more metallic character.

The peak positions of the UHB and LHB are progressively shifted further away from  $\pm U/2$  as  $N_{\text{deg}}$  increases. These shifts, roughly proportional to  $N_{\text{deg}} t^2/U$  for  $U$  sufficiently large, can be understood in terms of the perturbational contributions to energy levels with occupation numbers  $N_{\text{deg}} - 1$ ,  $N_{\text{deg}}$  and  $N_{\text{deg}} + 1$ , respectively. When  $t \approx U$ , one should also take into account this shift in addition to the band broadening at the MIT, which can complicate the argument of Gunnarsson, Koch, and Martin [5] that led to a  $\sqrt{N_{\text{deg}}}$  dependence to  $U_c$ .

The central peaks for  $N_{\text{deg}} = 2, 3$  are the quasi-particle (QP) excitation which emerges from the scattering of the spin degrees of freedom of conduction electrons. The width of the QP peak defines the new low temperature energy scale (renormalized Fermi energy). Since the spectral weight from the UHB and LHB is expected to be larger at  $\omega = 0$  for larger  $N_{\text{deg}}$  due to the broadening mentioned in a previous paragraph, the QP peak accordingly has larger weight at the chemical potential. This trend goes with enhanced metallicity for increasing  $N_{\text{deg}}$ . We will discuss more the dependency of the QP weight upon orbital degeneracy in relation to the electronic resistivity.

FIG. 2 (b) shows the one-particle spectral functions away from half-filling at  $U = 4, \epsilon_d = -1$  for all  $N_{\text{deg}}$ . In the paramagnetic phase, the total occupation number is evenly distributed among the orbitals and the spectral

weight of the LHB roughly goes as  $1/N_{\text{deg}}$ . Since  $|\epsilon_d| \ll U$  and the doubly occupied configuration exists in small quantum weight, total occupation number is not very sensitive to the orbital degeneracy.

The behavior of the MIT with a finite Hund's rule coupling  $J$  is shown in FIG. 3. When the exchange interaction  $J$  in Eq. (3) is included, the Coulomb repulsion is effectively increased, favoring the insulating phase. Numerical calculation confirms that the insulating phase is expanded with finite positive  $J$ . Figure 3 shows the plot of  $n_d$  vs.  $\epsilon_d - \epsilon_{ph}$  with  $J = 0.0, 0.2, 0.5, 1.0$  at  $N_{\text{deg}} = 2$  and  $\beta = 16$ . The total occupation number  $n_d$  begins to deviate from the half-filling value  $N_{\text{deg}}$  when the system become metallic.  $\epsilon_d$ 's where the metallic phases begin are pushed to higher values with  $\Delta\epsilon_d$  approximately linear in  $J$ . In other words, the insulating gap has increased with finite  $J$ .

The phenomena can be easily understood by considering the change in the on-site energy at half-filling. The effective on-site Coulomb repulsion  $U_{\text{eff}}$  can be computed as  $E(N_{\text{deg}} + 1) + E(N_{\text{deg}} - 1) - 2E(N_{\text{deg}})$  from the on-site Hamiltonian Eq. (3), which leads to

$$U_{\text{eff}} = U(N_{\text{deg}}, J = 0) + N_{\text{deg}}J, \quad \text{linear in } N_{\text{deg}}. \quad (4)$$

Also, we have to remember that the hopping of electrons leaves behind a trail of broken Hund's rule multiplets. Therefore, there would be additional effective repulsion due to hopping, which is ignored in Eq. (4). For  $A_3C_{60}$ ,  $J$  is one order of magnitude smaller than  $U$  [7], the Hund's rule coupling plays less important role than  $\sqrt{N_{\text{deg}}}U_c(1,0)$  in Eq. (1). For systems with larger  $J$ , one should take into account the last term in Eq. (3) to properly describe the magnetic correlation.

Finally, we discuss the transport properties of the MOHM. From the analytically continued one-particle spectral function, we can extract the electron scattering rate (imaginary part of the self-energy) and thereby calculate the optical conductivity,  $\sigma(\omega)$ , within the DMFT [15], as shown in FIG. 4. The inset (a) shows the evolution of spectral functions for a half-filled doubly degenerate model at inverse temperatures  $\beta = 2, 4, 8, 12, 16$ , where the curve with the large QP peak (labelled as  $a$  in the figure) corresponds to low  $T$ . The optical conductivities shown in the main plot are from the same set of temperatures. The optical conductivity is computed by convoluting the one-particle spectral functions and is therefore characterized by transitions between various single-particle excitations, as indicated in the figure. The Drude peak (marked as  $a - a$ ), resulting from the scattering *within* the QP peak  $a$ , diverges as the temperature goes to zero. Note that, since the leading order of  $\sigma(\omega)$  is  $O(1/d)$ , we have plotted  $d\sigma(\omega)$ .

The resistivity  $\rho(T)$ , plotted in inset (b), is calculated from the  $\omega \rightarrow 0$  limit of the optical conductivity,  $\rho(T)^{-1} = \lim_{\omega \rightarrow 0} \sigma(\omega)$ . The unit of  $\rho(T)/d$  is  $\mu\Omega\text{cm}$  [16]. The data shown here are for half-filled Hubbard models with double (filled circle) and triple (open circle) orbital

degeneracy at  $U = 4$  using the Gaussian free DOS with effective band width  $W = \sqrt{2}$ . The resistivity for doubly degenerate model shows a cross-over to a Fermi liquid behavior,  $\rho(T) \propto T^2$ , at low  $T$  from a resistivity of insulating character at high  $T$ . For the triply degenerate model, we could not determine the low temperature law of resistivity due to noise in QMC data.

It should be noted that  $\rho(T)$  for  $N_{\text{deg}} = 3$  is about one order of magnitude smaller than  $\rho(T)$  for  $N_{\text{deg}} = 2$ , in contrast to the weak  $N_{\text{deg}}$ -dependency in the low- $U$  perturbation theory [17]. Although not discussed in this paper, the magnitude of  $\rho(T)$  seems to strongly depend upon the shape of band edge of free DOS. For example, the resistivity for semi-circular DOS is order(s) of magnitude larger than for Gaussian DOS at the same  $U/W$  ratio. A systematic investigation of resistivity on the orbital degeneracy and DOS and its comparison with experiments are left for further studies.

We acknowledge an initial inspiration from T.M Rice to study this subject, along with useful discussions with H. R. Krishna-murthy, O. Gunnarsson. This work was supported in part by the U.S. Department of Energy, Office of Basic Energy Sciences, Division of Materials Research (J.H. and D.L.C.) and by National Science Foundation grant DMR-9704021 and DMR-9357199 (M.J.). Supercomputer time was provided by the Ohio Supercomputer Center.

- 
- [1] A. J. Millis, R. Mueller, and B. I. Shraiman, Phys. Rev. B **54**, 5389 (1996).
  - [2] T. M. Rice and M. Sigrist, J. Phys.: Condens. Matter **7**, L643 (1995), References therein.
  - [3] M. P. Gelfand, "Alkali fullerenes: Theoretical perspectives, progress and problems", in *Superconductivity Review* Vol. 1, p. 103, Gordon and Breach Science Publishers, 1994.
  - [4] O. Gunnarsson, Rev. Mod. Phys. **69**, 575 (1996); private communication.
  - [5] O. Gunnarsson, E. Koch, and R. M. Martin, Phys. Rev. B **54**, R11026 (1996).
  - [6] J. P. Lu, Phys. Rev. B **49**, 5687 (1994).
  - [7] R. W. Lof, M. A. van Veenendaal, B. Koopmans, H. T. Jonkman, and G. A. Sawatzky, Phys. Rev. Lett. **68**, 3924 (1992).
  - [8] H. Kajueter and G. Kotliar, Int. J. Mod. Phys. B **11**, 729 (1997).
  - [9] M. J. Rozenberg, Phys. Rev. B **55**, R4855 (1997).
  - [10] X.-D. Xiang, J. G. Hou, V. H. Crespi, A. Zettl, and M. L. Cohen, Nature **361**, 54 (1993).
  - [11] W. Metzner and D. Vollhardt, Phys. Rev. Lett. **62**, 324 (1989); Th. Pruschke, M. Jarrell and J.K. Freericks, Adv. in Phys. **42**, 187 (1995); A. Georges, G. Kotliar, W. Krauth, and M. J. Rozenberg, Rev. Mod. Phys. **68**, 13 (1996).

- [12] L. Dworin and A. Narath, Phys. Rev. Lett. **25**, 1287 (1970).  
[13] R. M. Fye and J. E. Hirsch, Phys. Rev. B **38**, 433 (1988).  
[14] M. Jarrell and J.E. Gubernatis, Physics Reports Vol. **269** No.3, p133-195, (May, 1996).  
[15] T. Pruschke, D. L. Cox, and M. Jarrell, Phys. Rev. B **47**, 3553 (1993).  
[16]  $\rho(T)/d = (\pi e^2/a^{d-2}\hbar)f(T/t^*, U/t^*, \epsilon_d/t^*)$  with the lattice constant  $a$ , and dimensionless  $f(T/t^*, U/t^*, \epsilon_d/t^*)$ . Here  $a$  is set to  $1\text{\AA}$  and  $d$  to 3.  
[17] O. Gunnarsson, Private Communication.

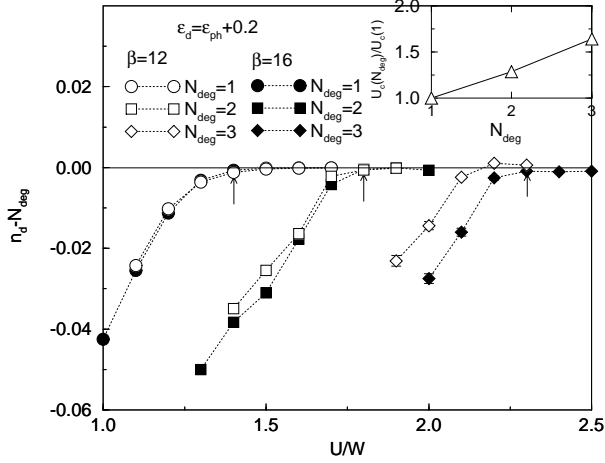


FIG. 1. The occupancy  $n_d$  versus the Coulomb repulsion  $U$  at fixed  $\epsilon_d = \epsilon_{ph} - (N_{deg} - \frac{1}{2})U + 0.2$ . The critical value of  $U$  (marked with arrows at  $T = 1/16$ ) at the cross-over between insulating and metallic solutions increased with  $N_{deg}$ . The temperature,  $T = 1/16$ , is not low enough for  $N_{deg} = 3$  case to equate the  $U_c = 2.3W$  as the zero-temperature quantum critical point. Due to the weak functional dependency of  $\sqrt{N_{deg}}$  and small  $N_{deg}$ , it is not clear that  $U_c(N_{deg}) = \sqrt{N_{deg}}U_c(1)$ . (See inset.) Lines are guide to the eye.

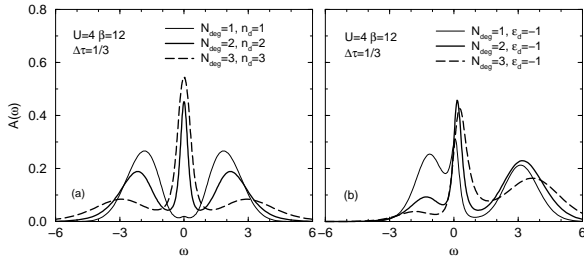


FIG. 2. Spectral functions for  $N_{deg} = 1, 2, 3$  at  $U = 4$  and  $J = 0$ . (a) The effective band-width of the charge excitation peaks (nearly at  $\pm U/2$  at half-filling) is broadened with increasing  $N_{deg}$  due to the enhanced hopping for one-particle (hole) doped states. The quasi-particle (QP) peak becomes dominant for large  $N_{deg}$ , as more weight of charge excitation peaks is transferred to the QP peak. (b) At a fixed  $\epsilon_d = -1$ , all three cases have total occupations near 0.9 and the integrated weight up to the chemical potential is roughly  $1/N_{deg}$ .

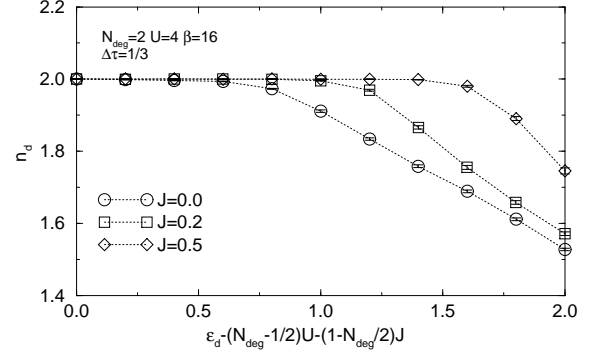


FIG. 3.  $n_d$  vs.  $\epsilon_d - \epsilon_{ph}$  at  $J = 0.0, 0.2, 0.5$ . For positive  $J$  the onset of a metallic solution is shifted to larger values of  $\epsilon_d$  from the particle-hole symmetric parameter,  $\epsilon_{ph}$ . The shift is roughly linear in  $J$ , leading to a suggestion that the on-site Coulomb interaction is responsible with  $\Delta U(J) = N_{deg} J$ .

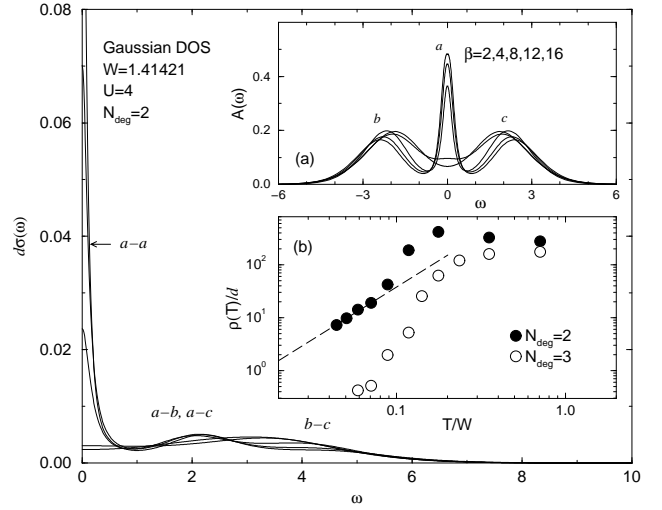


FIG. 4. Optical conductivity and resistivity for  $N_{\text{deg}} = 2$  at  $U = 4$ ,  $\epsilon_d = -1$ . The optical conductivity is made up of three excitations arising from transitions between three structures in the spectral functions plotted in the inset (a). The spectral functions at  $\beta = 2, 4, 8, 12, 16$  have QP peak, LHB, UHB marked as  $a, b, c$ , respectively. The Drude peak, arising from the scattering within the QP peak, becomes stronger as  $T$  lowers. The d.c. resistivity  $\rho(T)$  for the doubly degenerate-band Hubbard model (filled circle) illustrates that the Fermi liquid behavior (dashed line) holds at half-filling below the critical  $U$  value. The triply degenerate case (empty circle) has much lower values for the resistivity. The unit of  $\rho(T)/d$  in the figure is  $\mu\Omega\text{cm}$  [16].